BULLETIN OF THE POLISH ACADEMY OF SCIENCES
TECHNICAL SCIENCES, Vol. 67, No. 1, 2019
DOI: 10.24425/bpas.2018.125719

Determination of parameters for a design of the stable electro-dynamic passive magnetic support of a high-speed flexible rotor

T. SZOLC[1]*, K. FALKOWSKI[2], M. HENZEL[2], and P. KURNYTA-MAZUREK[2]

[1] Institute of Fundamental Technological Research of the Polish Academy of Sciences, Warsaw, Poland
[2] Faculty of Mechatronics and Aerospace of the Military University of Technology, Warsaw, Poland

Abstract. Electro-dynamic passive magnetic bearings are now viewed as a feasible option when looking for support for high-speed rotors. Nevertheless, because of the skew-symmetrical visco-elastic properties of such bearings, they are prone to operational instability. In order to avoid this, the paper proposes the addition of external damping into the newly designed vibrating laboratory rotor-shaft system. This may be achieved by means of using simple passive dampers that would be found among the components of the electro-dynamic bearing housings along with magnetic dampers, which satisfy the operational principles of active magnetic bearings. Theoretical investigations are going to be conducted by means of a structural computer model of the rotor-shaft under construction, which will take into consideration its actual dimensions and material properties. The additional damping magnitudes required to stabilize the most sensitive lateral eigenmodes of the object under consideration have been determined by means of the Routh-Hurwitz stability criterion.

Key words: rotor-dynamics, electrodynamic passive magnetic bearings, flexible rotor-shaft, active magnetic damper, stability analysis.

1. Introduction

Due to a significant increase in the nominal rotational speeds of rotating machinery (reaching 100,000 rpm or even more), the rolling element and the oil-film journal bearings, commonly applied to rotor-shafts till now, should be gradually replaced with more modern contact-less and lubricant-free supports. Consequently, several types of magnetic bearings have already been developed for high-speed rotating machines. Generally, these take the form of active magnetic bearings (AMB), which are known to possess several advantages as well as disadvantages. Other than their transverse load transmission ability, AMBs can also function as actuators for active control of rotor-shaft lateral vibrations. Nevertheless, they must be equipped with complex electronic control devices, which are usually characterized by massive coils of relatively large dimensions, making them problematic for a range of technical applications. Moreover, failures in control can result in a sudden and significant loss in stability. Thus, during the last 10–15 years, as a consequence of developments in electrical engineering, electronics and material technology, many types of passive magnetic bearings (PMB) have been developed, whose applications have steadily increased. These include: permanent magnet static magnetic bearings, superconductor passive magnetic bearings and electro-dynamic passive magnetic bearings (EDPMB). The physical fundamentals for a dynamic rotary passive magnetic levitation can be found in [1, 2]. Both a theoretical formulation of the problem and an experimental realization is presented in those. It is worth noting that in these papers mathematical modelling of passive magnetic levitation, based on the solution of Maxwell equations, leads to parallel action of the elastic and dissipative suspending forces. For small-size high-speed rotors, this approach has been applied in [3], where it results in theoretical and experimental development of radial EDPMBs, which are characterized by sleeve-shaped rotating conductors. With such a form of modelling, the suspension on the EDPMBs was compared for flexible rotor-shafts in [4] with analogous support provided by classical oil-journal bearings in an industrial centrifugal compressor as well as with the support provided by rolling bearings in a single-spool gas turbine. EDPMBs with disk-shaped conductors have further been modelled in [5] and [6] by applying Kirchhoff's voltage law to electrical circuits, including those generating resistance and self-inductance of the conductor. These assume linear proportionalities between the bearing levitation force and induced currents and between the electromotive force and the radial journal-to-bushing velocity. In this model, the magnetic levitation force is transmitted in a given direction by an elastic spring and a viscous damper connected with each other in series.

The EDPMBs possess crucial advantages over AMBs. Firstly, EDPMBs do not require a power supply and allow for resonant-free operation. Secondly, they have a relatively simple structure and, accordingly, are cheaper than AMBs. Nevertheless, EDPMBs possess several disadvantages. These include their limited load capacity for supporting big rotors and poor damping abilities at high rotational speeds. Furthermore, these bearings can quite often cause operational instability. In order to avoid this drawback and thus maintain the above-mentioned advantages, the introduction of additional external damping into the rotor-shaft system is necessary. This problem was first raised in [1, 2] and [3]. In [7], dynamic analysis has been performed for the suspension on AMBs combined with static PMBs, which are fitted to the rotor-shaft in order to stabilize its lateral vibrations. Static radial PMBs together with a thrust EDPMB have been investigated in [8] for a vertical rotor-shaft, where stabilization

*e-mail: tszolc@ippt.pan.pl

Manuscript submitted 2018-06-27, revised 2018-08-10, initially accepted for publication 2018-09-03, published in February 2019.

was provided by mechanical touch-down bearings. The rationale for inserting additional damping into a radial EDPMB supporting a rigid rotor is presented in [9] and [10], where they offer combined passive-active magnetic support for rigid rotor-shafts, as well as in [11], using external damping generated passively. Requirements for stable magnetic suspension of bearing-less synchronous motor rotors have been also investigated in [12].

According to the above, in order to assure sufficient stability limits for a newly designed rotor-shaft supported by the EDPMBs, appropriate dynamic analysis must first be carried out. One of the main goals of such a study is the selection of relevant sources of damping in the object being considered and determination of their respective dynamic parameters, in particular the proper values of damping coefficients. In the paper being presented, for the constructed laboratory flexible rotor-shaft suspended magnetically, several approaches are proposed to eliminate instability caused by the skew-symmetry of visco-elastic properties of the EDPMBs. These approaches may be summarized as an attempt to include additional external damping in the vibrating system to such an extent as to satisfy the Routh-Hurwitz stability criterion and to maintain all system eigenvalue real parts always negative. This is going to be achieved by means of passive damping (which is generated by the visco-elastic suspension of the bearing stators in their housings), by proper selection of the electro-dynamic bearing global stiffness, and by the use of active magnetic dampers (AMD).

2. Description and modelling of the bearing-rotor-shaft system

The investigations are going to be conducted for a newly designed laboratory multi-disk rotor-shaft, supported by two EDPMBs, No 1 and 2, as shown in Fig. 1. It consists of a relatively slender flexible stepped shaft with a total length of 0.813 m and with three heavy rotors attached. This rotating system has a total mass of 7.3 kg, and a bearing span equal to ca. 0.677 m; it operates within a rotational speed range of 0–55000 rpm. Such a structure is representative for a broad range of rotor machines currently being applied in the industry.

2.1. Modelling the rotor-shaft. In order to obtain sufficiently reliable results of the eigenvalue analysis for this rotor-shaft, all computations will be performed by means of the hybrid structural model consisting of continuous visco-elastic beam finite elements and discrete oscillators, as e.g. in [4, 13–15]. In an identical way as in the case of a classical discretized beam finite element formulation, the following points are taken into consideration when using such a model: the rotor-shaft geometry, its material properties, gyroscopic effects and shaft material damping, as described by the standard body model. In the hybrid model, successive cylindrical segments of the stepped rotor-shaft are represented by flexurally deformable cylindrical macro-elements of continuously distributed inertial-visco-elastic properties. With an accuracy that is sufficient for practical purposes, some heavy rotors can be substituted with rigid bodies attached to the macro-element extreme cross-sections.

Each bearing is represented by a dynamic oscillator possessing two degrees of freedom, in which apart from the magnetic field interaction, the visco-elastic properties of the bearing housing and foundation are also included. This bearing model makes it possible to represent, with relatively high accuracy, the kinetostatic and dynamic anisotropic and anti-symmetric properties in the form of constant or variable stiffness and damping coefficients. Moreover, the oscillator mass can correspond to inertia of the magnetic bearing stator's visco-elastically embedded in the bearing housing. Thus obtained mutual combination of continuous finite elements together with discrete oscillators and rigid bodies following the structure of real object results in the hybrid mechanical model. Figure 2 presents the

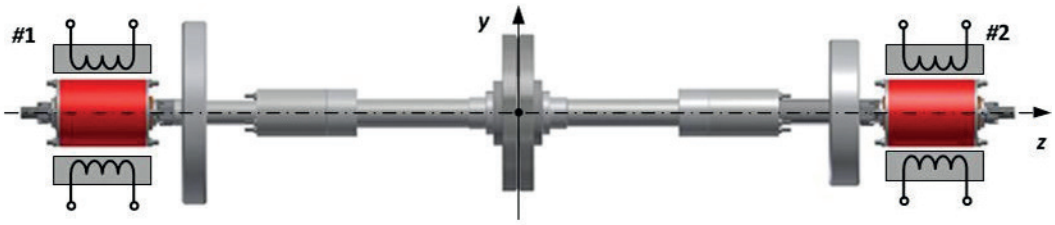

Fig. 1. Laboratory multi-disk rotor-shaft system

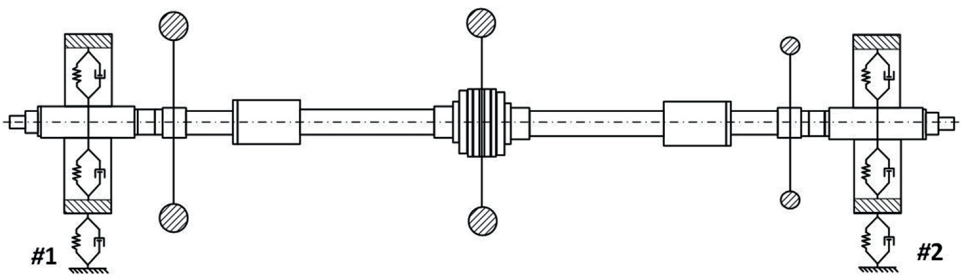

Fig. 2. Hybrid model of laboratory multi-disk rotor-shaft system

hybrid model of the laboratory rotor-shaft system in relation to which the postulated investigations will be carried out. Its stepped shaft has been divided into 46 cylindrical segments of lengths, diameters and material constants following from the technical documentation of the designed object.

2.2. Modelling the electrodynamic passive magnetic bearing. The principle of a radial EDPMB's operation can be reduced to mutual, non-contact interaction between a rotating conductor (at room temperature) and permanent magnets, thus creating a stator, as described in [3–6]. This is achieved by means of bearing support that consists of a conducting sleeve attached to the rotor-shaft journal and permanent magnets embedded in the bearing housing, as illustrated in Fig. 3. In order to assure a sufficiently high transverse load ability for such a bearing, the permanent magnets must be mutually placed and properly separated by the iron pole shoes in a manner resulting in the so-called heteropolar or homopolar type of the radial passive magnetic bearing ([3] and [6]). In the case of the heteropolar bearing, the magnetic field is sinusoidal just outside the border of the permanent magnets and its magnetic vector potential is perpendicular to the plane of the flux distribution. However, the homopolar bearing is characterized by radial flux distribution, which makes it more advantageous for practical engineering applications.

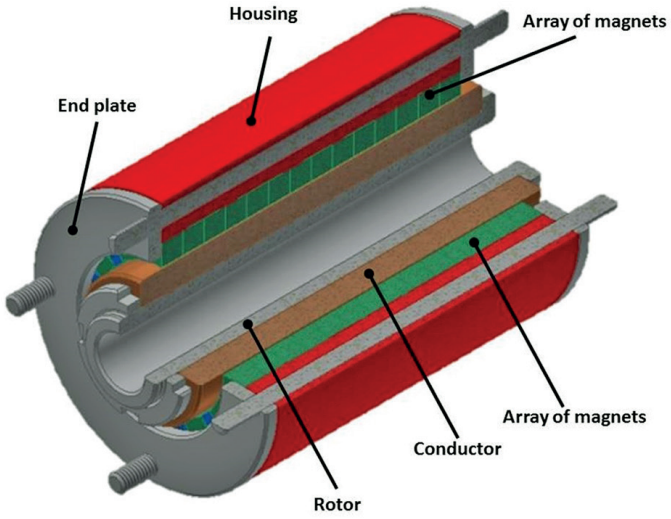

Fig. 3. Scheme of radial electrodynamic passive magnetic bearing

Here, dynamic modelling of the EDPMBs is intended to calculate their electromagnetic stiffness and damping characteristics. These quantities have been determined using fundamentals of the non-contact dynamically stabilized suspension theory, which utilizes a combination of static interaction between permanent magnets and dynamic interaction between room-temperature conductors and magnets [1]. For this purpose, as in [3], computations will be carried out for various rotational speeds by means of the advanced 3D finite element code, COMSOL Multiphysics. In the case being considered, the bearing's 'in plane' transverse global stiffness K can be defined as:

$$K(\Omega) = -\frac{\mathrm{d}F(\Omega)}{\mathrm{d}(\Delta r)}, \text{ where: } F(\Omega) = \int_V (J \times B)\mathrm{d}V \tag{1}$$

is the Lorenz force, J and B denote, respectively, the current volume and external magnetic flux densities, Δr is the journal-to-bushing radial proximity, as discussed in [3] and [4], and Ω denotes the current shaft rotational speed. Then, upon the numerical determination of global stiffness $K(\Omega)$ by means of formula (1), the main rotor and cross-coupling stiffness components have been calculated in the form of shaft rotational speed functions, also discussed in [3] and [4]:

$$\begin{aligned} k_{xx}(\Omega) &= k_{yy}(\Omega) = K(\Omega)\cos\theta \\ \text{and } k_{xy}(\Omega) &= K(\Omega)\sin\theta = -k_{yx}(\Omega), \end{aligned} \tag{2}$$

where K denotes the bearing's 'in plane' global stiffness, Ω is the current shaft rotational speed and $\theta = \arctan(R/\Omega L)$ is the so-called 'force angle' expressed as a function of the magnetic bearing coil resistance R and inductance L.

Figure 4a illustrates the rotor main and cross-coupling (cr.-c) stiffness characteristics, which have been determined using the applied finite element model of the EDPMB that suspends the above-mentioned multi-disk rotor-shaft within its entire operating rotational speed range. These plots are qualitatively identical with those obtained in [3] and [5] for the high-speed rotor machines, other than for the one investigated here. Moreover, it is worth noting that, in general, the two above-mentioned approaches to EDPMB modelling, described, respectively, in [1, 2] and [3] as well as in [5] and [6], result in qualitatively identical stiffness characteristics, in spite of the mutually different physical interpretations of elastic and viscous property connections, i.e. arranged, respectively, parallelly and in series.

According to [3] and [4], damping coefficients of the EDPMB have been calculated by means of the following formulae:

$$\begin{aligned} d_{xx}(\Omega) &= d_{yy}(\Omega) = k_{xy}(\Omega)/\Omega \\ d_{xy}(\Omega) &= -d_{yx}(\Omega) = k_{xx}(\Omega)/\Omega, \end{aligned} \tag{3}$$

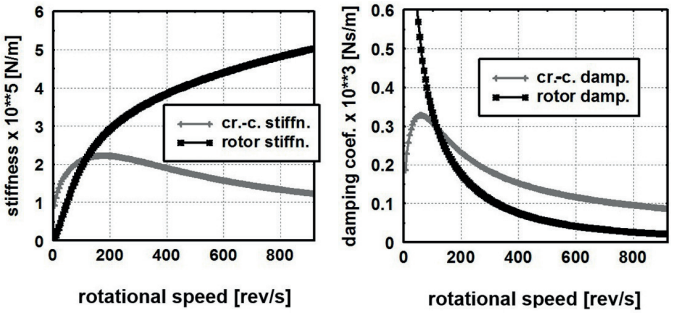

Fig. 4. Main (rotor) and cross-coupling (cr.–c) stiffness (a) and damping (b) characteristics of the EDPMB

where the main rotor and cross-coupling bearing stiffness components $k_{xx}(\Omega) = k_{yy}(\Omega)$ and $k_{xy}(\Omega) = -k_{yx}(\Omega)$ can be determined using formulae (2). The plots of the corresponding main and cross-coupling (cr.-c) damping coefficients for the EDPMB under consideration are presented in Fig. 4b.

The rotor-shaft system being considered here is expected to experience only small lateral displacements, i.e. ones that are much smaller than bearing clearance values, along with correspondingly small elastic deformations. Thus, neither geometrical nonlinearities nor so-called strong nonlinear effects, e.g. those caused by rubbings, are expected. According to the above, the mechanical model of this system has been assumed as linear with the bearing stiffness (2) and damping coefficients (3) regarded constant for given constant rotational speed values Ω.

3. Solution of the problem

The complete mathematical formulation and solution for the rotor-shaft system hybrid model applied here can be found e.g. in [13] and [14]. In this model, the flexural motion of cross-sections of each visco-elastic macro-element is governed by the partial differential equations derived using the Timoshenko and Rayleigh rotating beam theory. Such equations contain gyroscopic forces mutually coupling rotor-shaft bending vibrations in the vertical and horizontal plane. The analogous coupling effect caused by the system's rotational speed-dependent shaft material damping, described using the standard body model, is also taken into consideration. The solution for the bending vibration analysis has been obtained using the analytical-computational approach demonstrated in detail in [13, 14] and applied e.g. in [15]. In the case being considered, it is to emphasize that since, according to formulae (2) and (3), the visco-elastic bearing support parameters are rotational speed-dependent, the fundamental dynamic properties of the rotor-shaft, e.g. its natural frequencies, eigenfunctions, modal masses and others, also depend on the shaft rotational speed value Ω. But for a constant Ω in time, numerical values of all these quantities are also constant. Thus, for each Ω one can solve the differential eigenvalue problem for the orthogonal system. Then, an application of the Fourier solutions in the form of fast convergent series in orthogonal eigenfunctions leads to the following set of modal equations:

$$\mathbf{M}(\Omega)\cdot\ddot{\mathbf{r}}(t) + \mathbf{C}(\Omega)\cdot\dot{\mathbf{r}}(t) + \mathbf{K}(\Omega)\cdot\mathbf{r}(t) = 0, \tag{4}$$

where: $\mathbf{C}(\Omega) = \mathbf{C}_0(\Omega) + \Omega\cdot\mathbf{C}_g(\Omega)$
and $\mathbf{K}(\Omega) = \mathbf{K}_0(\Omega) + \mathbf{K}_b(\Omega) + \Omega\cdot\mathbf{K}_d(\Omega)$.

The symbols $\mathbf{M}(\Omega)$ and $\mathbf{K}_0(\Omega)$ denote, respectively, the rotational speed dependent diagonal modal mass and stiffness matrices, $\mathbf{C}_0(\Omega)$ is the non-symmetrical damping matrix containing the damping coefficients (3) of the passive magnetic bearings and $\mathbf{C}_g(\Omega)$ denotes the skew-symmetrical matrix of gyroscopic effects. Skew or non-symmetrical elastic properties of the bearings are described by matrix $\mathbf{K}_b(\Omega)$. Anti-symmetrical effects due to the standard body material damping model of the rotating shaft are expressed by the skew-symmetrical matrix $\mathbf{K}_d(\Omega)$. Of course, because of the reasons mentioned above, for given constant values of Ω all these matrices are regarded constant. The modal coordinate vector $\mathbf{r}(t)$ consists of the unknown time functions standing in the Fourier solutions. The number of equations (4) corresponds to the number of bending eigenmodes taken into consideration in the frequency range of interest.

Since the main target of the study being carried out is an investigation of stability of the considered rotating system, regarded here as a linear one, its eigenvalue real parts are going to be regarded first as the fundamental measure of asymptotic stability. In order to determine eigenvalues of the rotor-shaft dynamic model, it is convenient to transform its modal motion equations (4) into analogous equations in the modal state co-ordinates:

$$\mathbf{A}(\Omega)\cdot\dot{\mathbf{x}}(t) + \mathbf{B}(\Omega)\cdot\mathbf{x}(t) = \mathbf{0}, \tag{5}$$

where:

$$\mathbf{A}(\Omega) = \begin{bmatrix} \mathbf{0} & -\mathbf{M}(\Omega) \\ \mathbf{M}(\Omega) & \mathbf{C}(\Omega) \end{bmatrix},$$

$$\mathbf{B}(\Omega) = \begin{bmatrix} \mathbf{M}(\Omega) & \mathbf{0} \\ \mathbf{0} & \mathbf{K}(\Omega) \end{bmatrix}, \quad \mathbf{x}(t) = \begin{bmatrix} \dot{x}(t) \\ x(t) \end{bmatrix}$$

and $\mathbf{x}(t)$ denotes the modal state vector. Assuming the well-known exponential complex analytical solution for (5), one obtains a system of $2n$ homogeneous algebraic equations which can be finally transformed into the following form:

$$\left(\mathbf{D}(\Omega) - \lambda\cdot\mathbf{I}\right)\cdot\mathbf{X} = \mathbf{0}, \tag{6}$$

where $\mathbf{X}$ and λ are, respectively, the complex eigenvector and eigenvalue of the hybrid mechanical model of the rotating system, $\mathbf{I}$ is the identity matrix, n denotes the number of orthogonal eigenmodes considered in (4) and matrix $\mathbf{D}$ is equal to:

$$\mathbf{D} = \begin{bmatrix} \mathbf{0} & \mathbf{I} \\ \dfrac{\mathbf{K}_0(\Omega) + \mathbf{K}_b(\Omega) + \Omega\cdot\mathbf{K}_d(\Omega)}{-\mathbf{M}(\Omega)} & \dfrac{\mathbf{C}_0(\Omega) + \Omega\cdot\mathbf{C}_g(\Omega)}{-\mathbf{M}(\Omega)} \end{bmatrix}. \tag{7}$$

It is to emphasize that the non-symmetry of the modal damping submatrix $\mathbf{C}_0(\Omega)$ as well as the skew-symmetry of the gyroscopic matrix $\mathbf{C}_g(\Omega)$ and skew-symmetry of both modal stiffness submatrices $\mathbf{K}_d(\Omega)$ and $\mathbf{K}_b(\Omega)$ can very distinctly influence dynamic stability properties of the entire rotor-shaft system. Because matrix $\mathbf{D}$ is a non-symmetrical one, in order to effectively determine the complex eigenvalues from (6), it is necessary to reduce it to the Hessenberg form using the Householder transformation. Then, the final computation of the eigenvalue real and imaginary parts for each bending eigenmode of the considered system is achieved by means of the commonly known QR algorithm.

4. Stability analysis

In order to assess the sufficient magnitude of additional damping necessary to eliminate the instabilities caused by EDPMBs that support the newly constructed laboratory rotor-shaft system, thorough dynamic stability analysis of this object should be carried out first. Such analysis will be performed using the hybrid model of the rotor-shaft under consideration within a frequency range of 0–1000 Hz, which includes 13 bending eigenforms. Investigations were conducted for the bearing visco-elastic characteristics (depicted in Fig. 4) in the above-mentioned rotational speed range of 0–55000 rpm, which corresponds to 0–920 rev/s. Figure 5 illustrates plots of the imaginary parts of system eigenvalues expressed as rotational speed functions.

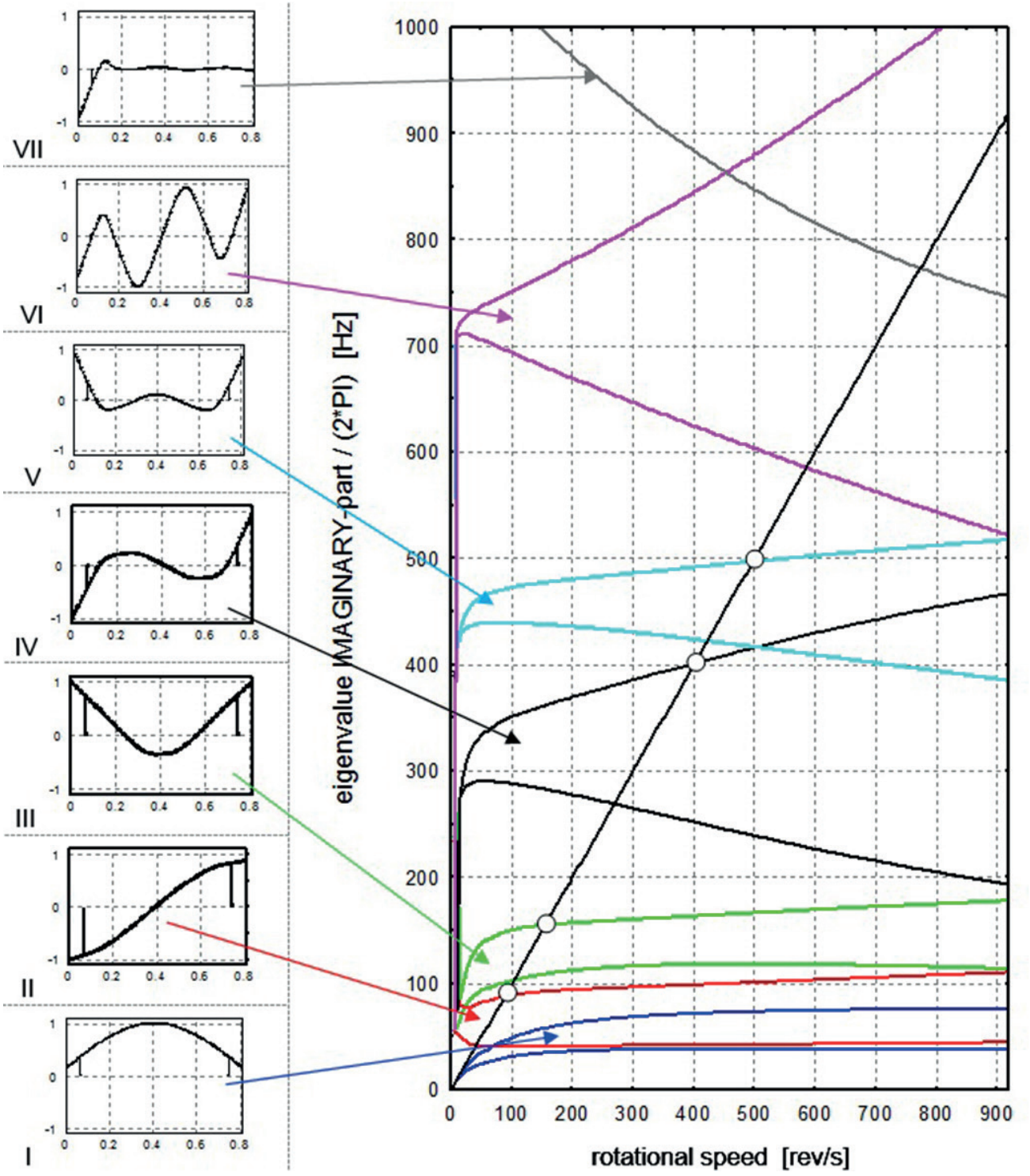

Fig. 5. Eigenvalue imaginary parts of the rotor-shaft supported on EDPMBs

Since these functions play the role of damped natural frequencies ω_{Di}, $i = 1, 2,\ldots, 13$, their illustration in this Figure takes the form of the Campbell diagram with marked critical speeds that correspond to forward whirls of successive eigenforms. For greater clarity, the respective bending eigenfunctions are depicted on the left-hand side. This is to emphasize here that, as mentioned above, for successive constant rotational speeds Ω, the system modal motion equations (4) and motion equations (5) in the modal state co-ordinates are linear. Then, the critical speeds of the first type can be defined only for external excitation frequencies coinciding with the rotor-shaft natural frequencies. In the case being considered, synchronous excitation due to usually unavoidable residual unbalances seems to be most representative. Figure 6 illustrates, in an analogous

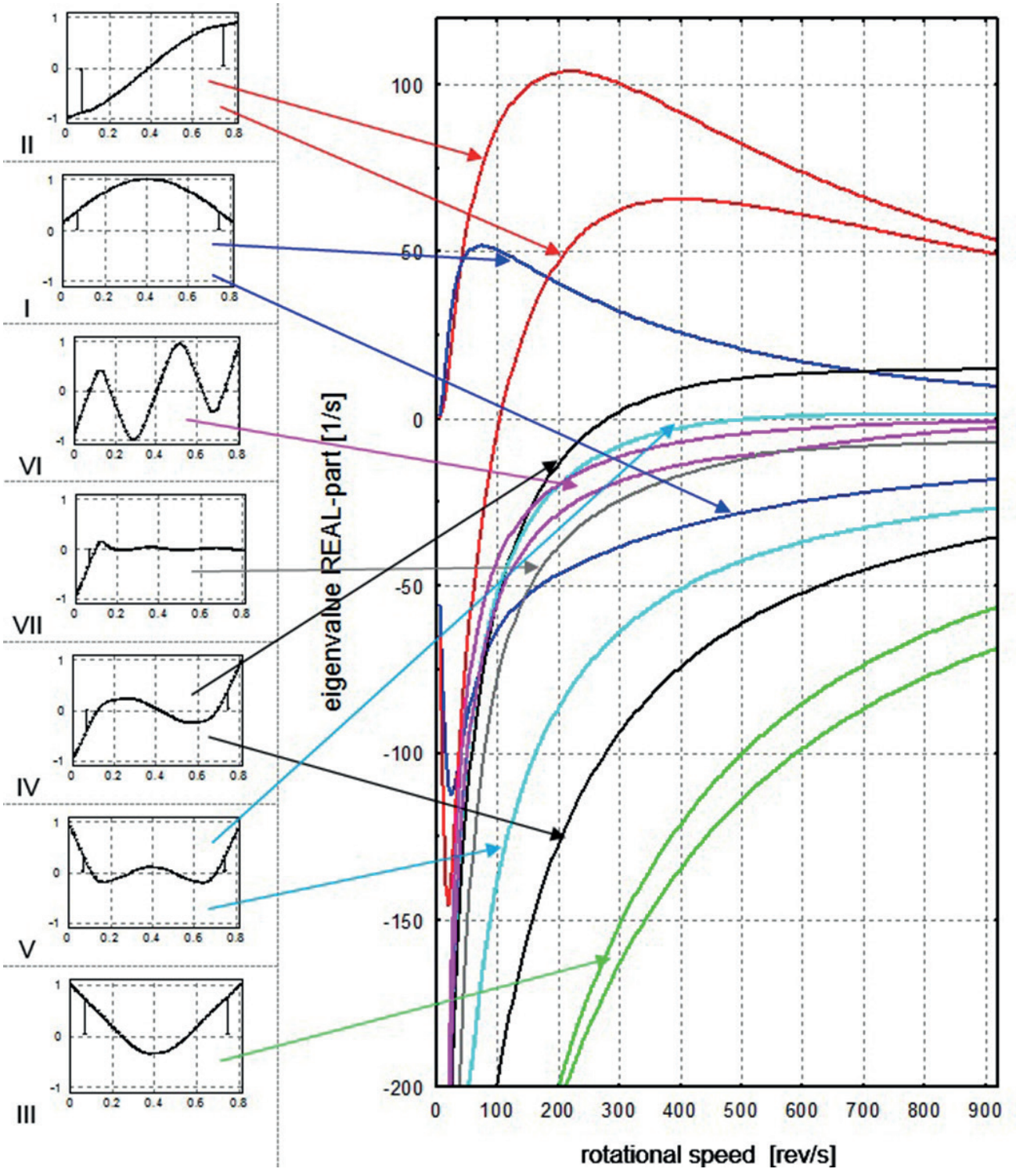

Fig. 6. Eigenvalue real parts of the rotor-shaft supported on EDPMBs

manner, the real parts μ_i, $i = 1, 2,\ldots, 13$, of the rotor-shaft eigenvalues. From the plots illustrated in this Figure, it follows that not all of the eigenvalue real parts are negative, which results in instability of the rotating system. This is most noticeable in those real parts that correspond to all precessions of the second eigenform; to the backward precession of the first eigenform, to the backward precession of the fourth eigenform and to the backward precession of the fifth eigenform, when it has rotational speeds greater than 500 rev/s, see Fig. 6.

5. Application of Routh-Hurwitz stability criterion

In order to avoid this negative consequence of using EDPMBs, it is necessary to introduce an adequate amount of additional damping into the system. By means of eigenvalue analysis, arbitrarily complex linear rotating systems can be investigated, and their asymptotic stability limits can be effectively determined. In order to find the sufficient additional damping magnitude required to stabilize the rotor-shaft system, it would be necessary to apply the trial-and-error quantitative approach, which is rather troublesome in computational practice. Consequently, for this purpose, the Routh-Hurwitz stability criterion is very convenient, but it can only be used effectively for rather simple linear rotor-shaft models. Here, as can be seen from the results of eigenvalue analysis demonstrated in Fig. 6, the fundamental eigenforms, similar in shape to cylindrical and conical ones, are most sensitive to instability. Thus, in order to obtain a rough estimation of additional damping magnitude, necessary to stabilize the first, 'quasi-cylindrical' eigenmode of the rotor-shaft being considered, the Routh-Hurwitz stability criterion leads to the following formula:

$$d_{\text{stab}} > \sqrt{mK}\,\frac{\sin\theta}{\sqrt{\cos\theta}} \tag{8}$$

derived in [1, 2] for the passive magnetic levitation of the rotating disk. This inequality has also been used in [3] for the Jeffcott rotor suspended by radial EDPMBs, and thus it can be applied for stabilizing cylindrical eigenmodes of symmetrical rigid rotors, when this type of magnetic support is used. In the case considered here, m is the rotor mass levitated by one bearing of the rotor-shaft depicted in Fig. 1 and regarded as semi-rigid and symmetrical. The global stiffness K and the force angle θ standing in (8) have already been defined in formulae (1) and (2).

Expression (8) was originally determined assuming that coefficients (3) of damping generated by the EDPMB are negligibly small, especially in the case of high rotational speeds Ω. Then, d_{stab} denotes the coefficient of additional rotor-to-stator damping expected to assure stable dynamic behavior of the rotating system. Bearing in mind that the EDPMB generates some damping which stabilizes rotor lateral vibrations, albeit insufficiently, i.e. the main rotor damping with coefficients $d_{xx} = d_{yy}$ defined by (3) and illustrated in Fig. 4b, the actual damping coefficient that is expected to stabilize the rotor-shaft cylindrical mode can be expressed as:

$$\begin{aligned} &d_{\text{stab}} - d_{xx} = d_{\text{stab}} - d_{yy} = d_{\text{add}} \;\text{ if }\; d_{\text{stab}} - d_{xx} \geq 0 \\ &\text{or }\; d_{\text{add}} = 0 \;\text{ if }\; d_{\text{stab}} - d_{xx} < 0. \end{aligned} \tag{9}$$

As follows from relationships (2, 3, 8), the damping coefficients d_{stab} and $d_{xx} = d_{yy}$ are proportional to global stiffness K of the EDPMB. This means that the 'softer' the bearing, the less damping is necessary to stabilize the cylindrical eigenmode of the rotor-shaft. Figure 7, by the black thick line, plots the characteristic of the additional damping coefficient d_{add} expressed as a function of shaft rotational speed Ω. This is obtained for 'nominal' global stiffness $K(\Omega)$, for which the results illustrated in Fig. 4, 5 and 6 have been determined. The analogous characteristic of d_{add} computed for the two-fold smaller bearing global stiffness, i.e. for $K(\Omega)/2$, is marked by the grey thick line in Fig. 7. In order to compare the influence of the bearing global stiffness on the characteristics of d_{add}, using the black and grey thin lines in Fig. 7, analogous plots, obtained respectively for $K(\Omega)/4$ and for $2K(\Omega)$, are included. From this comparison, it follows that the global stiffness realized by the EDPMB has a crucial influence on the required values of the additional damping coefficient d_{add}, above which stabilization of the rotor semi-cylindrical vibration mode can be expected. It is necessary to emphasize that all the rotational speed values, at which the maxima of the additional required damping coefficient d_{add} occur, are contained within the range of Ω corresponding to the greatest positive eigenvalue real parts calculated for the rotor-shaft under consideration, see Fig. 6 and 7.

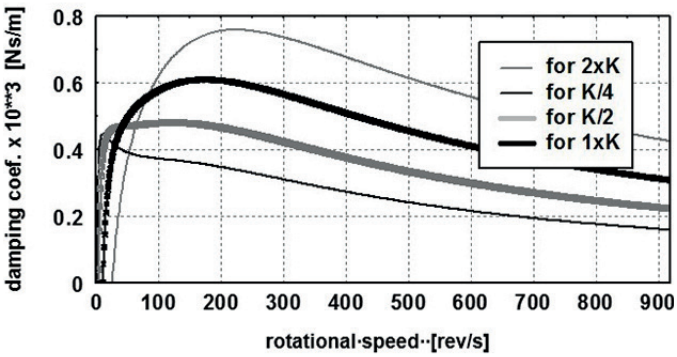

Fig. 7. Characteristics of minimum values of coefficients d_{add} of additional damping necessary to stabilize the rotor-shaft cylindrical mode

Nevertheless, it is more difficult to stabilize the conical mode of this rotor-shaft, and determination of the analogous additional damping coefficient using the Routh-Hurwitz criterion requires separate analysis. From general equations of motion of rigid rotors suspended by two bearings, e.g. in [16], it follows that in the case of symmetrical rotors the cylindrical and conical motions are mutually uncoupled. Then, these motion equations can be split into two separate sub-sets describing both trans-

lational and rotational movements. Acting in accordance with the Hurwitz procedure, which is presented in detail in [17], it is necessary to transform the two-degrees-of-freedom subsystem of equations, describing the rigid rotor-shaft conical motion, into a first order form with the following matrix **E** containing the inertial-visco-elastic coefficients:

$$\mathbf{E} = \begin{bmatrix} 0 & 1 & 0 & 0 \\ -2l^2\frac{k}{I} & -2l^2\frac{c_{stab}}{I} & -2l^2\frac{s}{I} & \frac{2l^2 d + \Omega I_0}{I} \\ 0 & 0 & 0 & 1 \\ 2l^2\frac{s}{I} & -\frac{2l^2 d + \Omega I_0}{I} & -2l^2\frac{k}{I} & -2l^2\frac{c_{stab}}{I} \end{bmatrix}, \quad (10)$$

where $2l$ denotes the bearing span, while $k = k_{xx}(\Omega) = k_{yy}(\Omega)$, $s = k_{xy}(\Omega) = -k_{yx}(\Omega)$ and $d = d_{xy}(\Omega) = -d_{yx}(\Omega)$, and have already been defined in (2–3). For our rotor-shaft $I_0 = 9.76 \cdot 10^{-3}$ kgm^2 and $I = 0.341$ kgm^2 are, respectively, its polar and diametral mass moments of inertia. Symbol c_{stab} denotes the coefficient of damping expected to assure a stable conical motion in an analogous sense as coefficient d_{stab} in inequality (8). Performing the successive steps of the Hurwitz procedure, in the case under study the stability criterion can be achieved for the damping coefficients c_{stab} present in matrix **E**, if the following inequality is satisfied:

$$\begin{aligned} &c_{stab}^4 - \left(d - \frac{\Omega I_0}{2l^2}\right)\frac{s}{k}\cdot c_{stab}^3 + \\ &+ \left[\left(d - \frac{\Omega I_0}{2l^2}\right)^2 - \frac{I}{2l^2}\frac{s^2}{k}\right]\cdot c_{stab}^2 - \\ &- \left(d - \frac{\Omega I_0}{2l^2}\right)^3 \frac{s}{k}\cdot c_{stab} - \left(d - \frac{\Omega I_0}{2l^2}\right)^2 \frac{I}{2l^2}\frac{s^2}{k} > 0. \end{aligned} \quad (11)$$

Similarly, as for the cylindrical eigen vibration mode of the rigid rotor-shaft, the actual damping coefficient expected to stabilize the conical mode can be expressed as:

$$\begin{aligned} &c_{\text{stab}} - d_{xx} = c_{\text{stab}} - d_{yy} = c_{\text{add}} \ \text{ if } \ c_{\text{stab}} - d_{xx} \geq 0 \\ &\text{or } \ c_{\text{add}} = 0 \ \text{ if } \ c_{\text{stab}} - d_{xx} < 0. \end{aligned} \quad (12)$$

The black lines in Fig. 8 plot characteristics of the stabilizing additional damping coefficients, expressed as functions of shaft rotational speed Ω. These have been obtained for 'nominal' global stiffness $K(\Omega)$. Here, the thick line corresponds to coefficient c_{add}, which is responsible for stabilization of the conical mode. For comparison, the thin line (reproduced from Fig. 7) corresponds to coefficient d_{add} of damping expected to stabilize the cylindrical mode. The analogous characteristics of c_{add} and d_{add} computed for the two-fold smaller bearing global stiffness $K(\Omega)/2$ have been marked in Fig. 8 by the grey thick and grey thin line, respectively. From the plots depicted in this

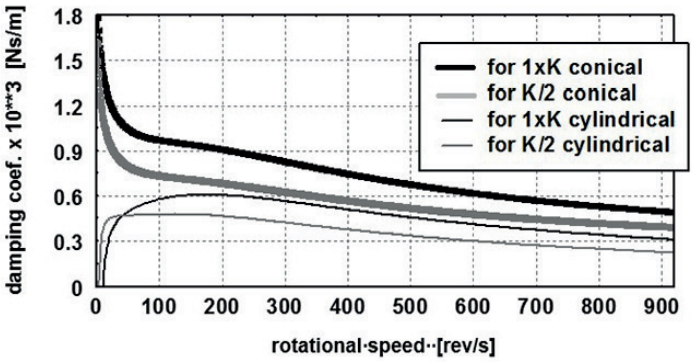

Fig. 8. Characteristics of minimum values of coefficients c_{add} and d_{add} of additional damping necessary to stabilize the rotor-shaft conical and cylindrical mode

Figure, it follows that stabilization of the rotor-shaft conical mode requires significantly more additional damping than that necessary for the cylindrical mode. This is particularly the case for the small and very small shaft rotational speeds, for which c_{add} are extremely high.

6. Stabilization of rotor-shaft supported on EDPMBs

Since the main causes of the observed instability are the skew-symmetrical visco-elastic properties of the EDPMBs (see formulae (2–3)), additional stabilizing external damping should be applied**.** For this purpose, a combined magnetic bearing is proposed that consists of main passive electrodynamic shaft support and of a magnetic damper, which is characterized by a relatively 'soft' elastic property and a potentially high ability of mechanical energy dissipation. In such a combined bearing, four additional independent windings are installed, together with ferromagnetic cores that create actuators which will generate magnetic forces acting in two mutually perpendicular directions, as shown in Fig. 9a, b. The temporary values of these forces are determined by the controller, which properly interprets the signals received from the eddy current sensors measuring relative rotor-to-stator displacements. It is necessary to emphasize that in order to effectively attenuate rotor-shaft lateral vibrations, the controller must be capable of distinguishing between information received from measured displacements whose components vary slowly and quickly. This goal can be achieved if, for the magnetic damper, the PD active control strategy is applied. Such a concept of the magnetic damper enables us to better control the operation of this additional visco-elastic levitation, making it relatively cheap and easy to maintain and more electric energy saving. It is worth commenting on the fact that this method retains the obvious advantages of the fundamental electro-dynamic passive nature of the operation while, at the same time, minimizing the disadvantages often associated with active magnetic suspensions.

According to fundamentals of the AMB operation given e.g. in [18], when using the PD control, such a suspension can be

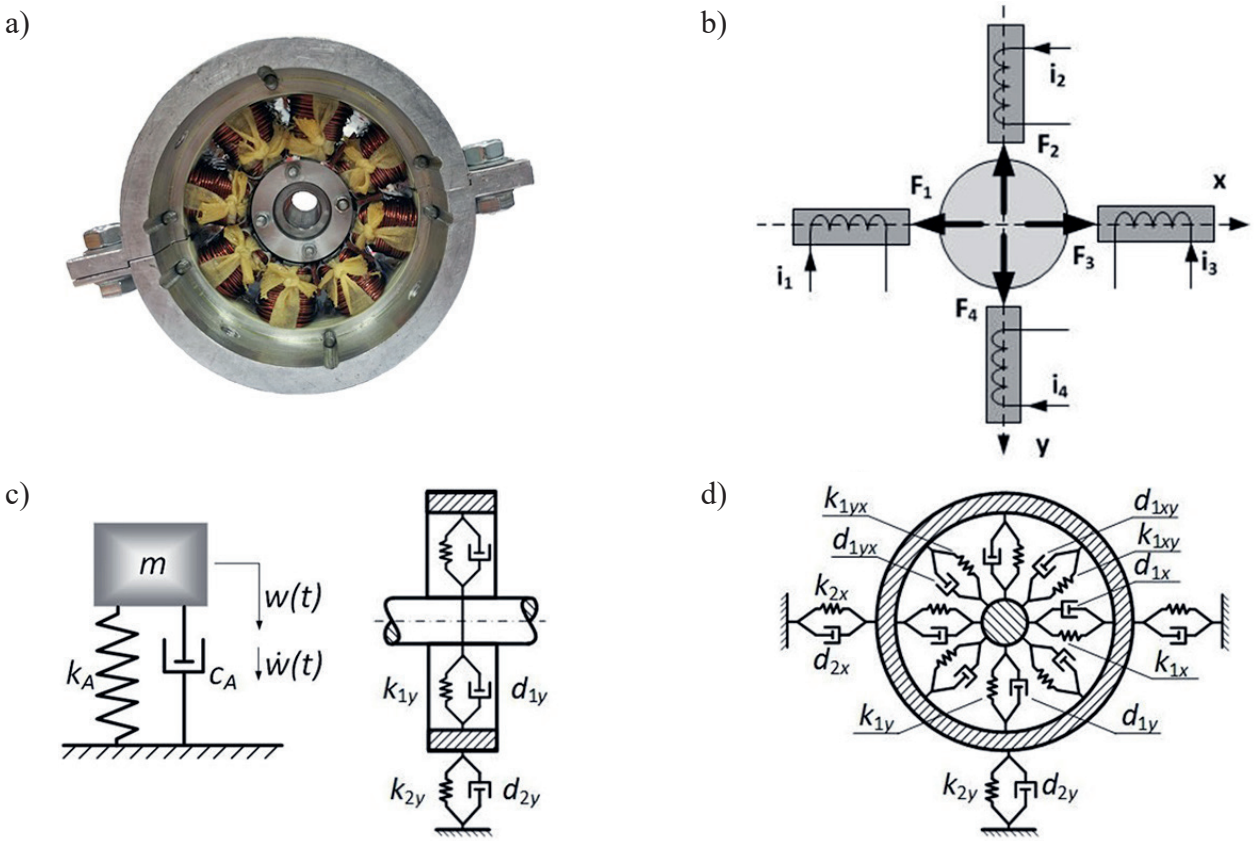

Fig. 9. AMD: real object (a), schematic view (b), mechanical model of the AMD (c) and bearing mechanical model (d)

interpreted as a single-degree-of-freedom dynamic oscillator shown in Fig. 9c. For computational purposes, stiffness k_A and damping coefficient c_A of this oscillator are determined by means of the following relationships:

$$k_A = m \cdot \omega_0^2 \quad \text{and} \quad c_A = 2m \cdot \gamma \cdot \omega_0, \tag{13}$$

where m denotes the part of the rotor-shaft mass supported by a given bearing, γ is the dimensionless factor of damping realized by active magnetic suspension and ω_0 denotes the oscillator natural frequency which can be calculated using the following expression:

$$\omega_0 = \frac{|\ln(\beta)|}{t_r \cdot \gamma}, \tag{14}$$

where t_r is the settling time, during which the perturbed signal will reach the expected steady-state value with the commonly used accuracy tolerance ratio $\beta = 0.04$, [18], as illustrated in Fig. 10.

Since the passive and active parts of the combined magnetic bearing act parallelly and in relatively close proximity to each other, the main rotor stiffness components $k_{xx}(\Omega)$ and $k_{yy}(\Omega)$, expressed in (2) and illustrated in Fig. 9d, become increased in their directions by stiffness k_A. Similarly, the main rotor damping coefficients $d_{xx}(\Omega)$ and $d_{yy}(\Omega)$ in (3) also become increased in their directions by damping coefficients c_A of the AMD. This way, additional stiffness and damping have been introduced to act between the rotor and bearing stator. When the proposed AMDs built into each EDPMB are applied, for the control gains corresponding to $t_r = 0.02$ s and $\gamma = 0.5$, additional stiffness $k_A = 3.74 \cdot 10^5$ N/m and damping coefficient $c_A = 1168$ Ns/m are introduced into both bearing supports. Consequently, almost all of the rotor-shaft's bending eigenmodes have been stabilized with the exception of the second one, as

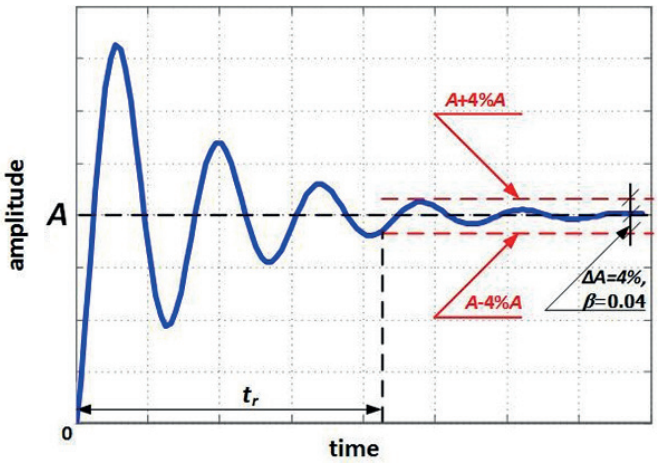

Fig. 10. Graphical demonstration of the mechanical energy dissipation ability realized by the AMD

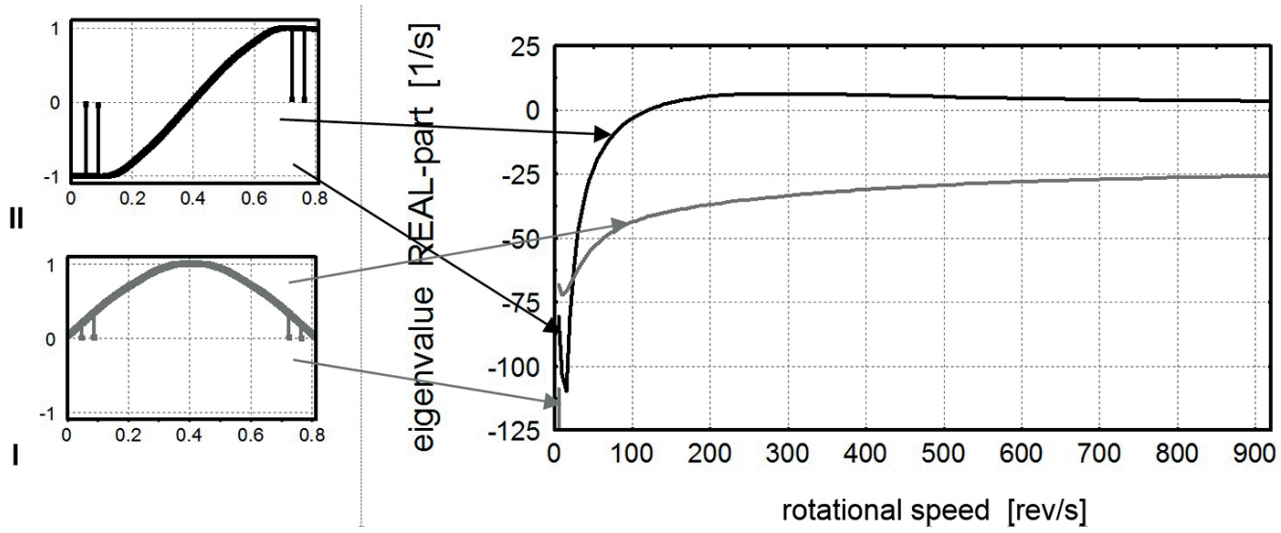

Fig. 11. Eigenvalue real parts determined for $t_r = 0.02$ s and $\gamma = 0.5$

follows from the respective plots demonstrated in Fig. 11. Here, the maximum value of the corresponding eigenvalue real part $\mu_{\max}$ is positive and equal to +6.23 1/s. In order to explain the result in this example, the Routh-Hurwitz criterion for determination of the minimum additional damping coefficient which is required for the stabilization of the conical and cylindrical modes has been applied. In this case, for the assumed hard 'metal-to-metal' embedding of the EDPMBs in their housings, it was necessary to take into consideration the stiffening effect caused by the additional constant stiffness k_A generated by the AMDs. Figure 12a presents the respective characteristics of minimum stabilizing, i.e. additional damping coefficients c_{add} and d_{add} that correspond to the conical and cylindrical modes. From these plots it follows that this additional stiffening significantly reduces the values of c_{add} for small and very small shaft rotational speeds Ω in comparison with the analogous characteristic depicted in Fig. 8. Nevertheless, the maximum of required $c_{\text{add}}(\Omega)$ in Fig. 12a reaches almost 1300 Ns/m and thus $c_A = 1168$ Ns/m generated by the AMDs turns out to be insufficient to stabilize the rotor-shaft completely.

In fact, all eigenmodes would become stable if the values of stiffness k_A and damping coefficient c_A of the AMDs were dominant in comparison with the main stiffness and damping components generated by the EDPMB, respectively. However, this would lead to typical active magnetic support and, consequently, the potential advantages from using PMBs would be lost. Hence, in order to introduce greater magnitude of passive damping into the vibrating rotor-shaft system, the hard 'metal-to-metal' embedding of the EDPMBs in their housings has been substituted by relatively soft visco-elastic interfaces in the form of layers made of vulcanized rubber or polymer foil. Stiffness and damping coefficient values of layers made of such materials have been determined using proper guidelines from [19] and [20]. Figure 12b illustrates the characteristics of minimum stabilizing additional damping coefficients c_{add} and d_{add} corresponding, respectively, to the conical and cylindrical

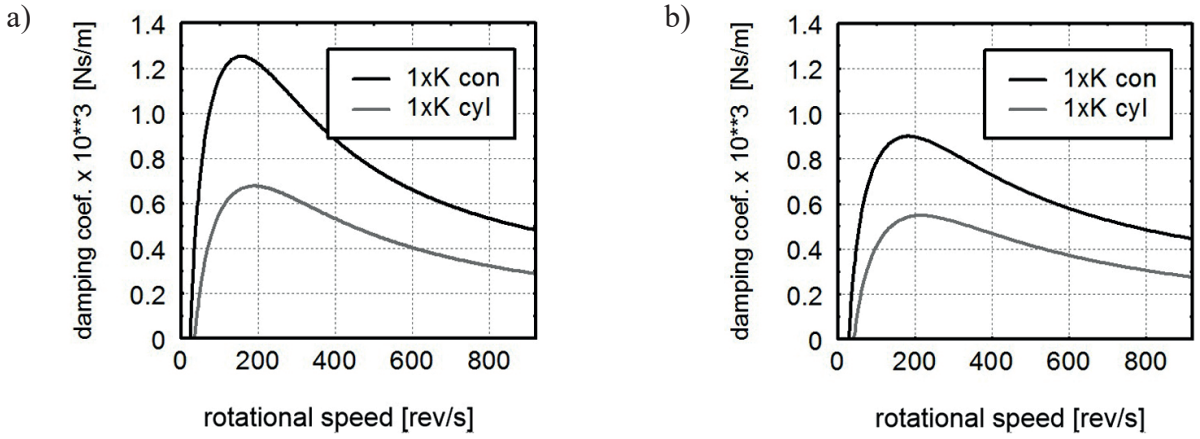

Fig. 12. Characteristics of minimum stabilizing additional damping coefficients c_{add} and d_{add} determined for global stiffness K and for embedding by means of 'metal-to-metal' (a) and with vulcanized rubber (b)

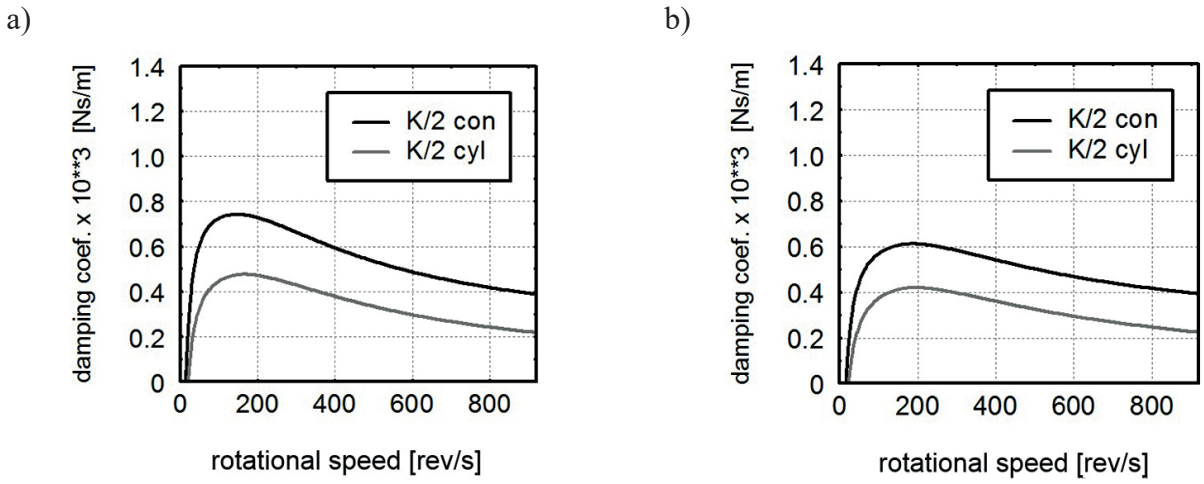

Fig. 13. Characteristics of minimum stabilizing additional damping coefficients c_{add} and d_{add} determined for global stiffness $K/2$ and for embedding with vulcanized rubber (a) and with polymer foil (b)

modes that have been obtained for the assumed embedding of the EDPMBs by means of layers of hard vulcanized rubber. Any consequent additional passive damping results in much lower values of c_{add} and d_{add} seen in comparison with those plotted in Fig. 12a. Thus, the maximum of $c_{add}(\Omega)$ in Fig. 12b required to stabilize the conical mode amounts to ca. 900 Ns/m and is considerably less than the $c_A = 1168$ Ns/m generated by the AMDs for the above-mentioned $t_r = 0.02$ s and $\gamma = 0.5$. The rotor-shaft system would be stabilized much more easily if the choice of global stiffness K of the EDPMBs was smaller. Then, according to (2–3), all the bearing stiffness and damping coefficient components decrease in proportion to one another. This fact has already been indicated above, using the Routh-Hurwitz stability criterion, resulting in the plots presented in Fig. 7 and 8. Hence, the stabilization effect can be obtained for relatively smaller values of additional damping coefficients c_{add} and d_{add} determined by means of formulae (8–9) and (11–12). Consequently, in order to stabilize a given rotor-shaft supported on the EDPMBs, respectively lower values of k_A and c_A realized by the AMDs can be applied. Less control energy will be consumed this way, and the entire control mechanism will weigh less and have smaller dimensions. For two-fold smaller stiffness and damping coefficient components than those plotted in Fig. 4, i.e. for half the bearing global stiffness $K(\Omega)/2$, Fig. 13 illustrates characteristics of minimum stabilizing additional damping coefficients c_{add} and d_{add} corresponding to the conical and cylindrical modes. Fig. 13a presents the characteristics obtained for EDPMBs embedded in their housings by means of hard vulcanized rubber and Fig. 13b illustrates analogous plots that have been determined for an embedding by means of soft polymer layers. It is worth noting that in both cases the minimum values of the additional damping coefficients necessary to stabilize the rotor-shaft being investigated are much lower than those plotted in Fig. 12. Namely, the maximum of c_{add} does not exceed 750 Ns/m (see Fig. 13a) or it reaches 600 Ns/m only (see Fig. 13b) in the case of the EDPMBs embedded, respectively, in vulcanized rubber and using soft polymer layers.

Table 1 presents combined properties and numerical parameters corresponding to the six stabilization examples performed for the investigated rotor-shaft system. In the Table, proper numerical values of stiffness and damping coefficients k_{2x}, d_{2x}, k_{2y} and d_{2y} marked in Fig. 9d, demonstrating the bearing mechanical model, are assigned to the considered types of bearing stator embedding layers in housings, contained in the second column.

Table 1
Stabilization results for various rotor-shaft-bearing system parameters

Embedding layer		Glob. stiffn.	t_r [s]	γ [–]	k_A [N/m]	c_A [N/m]	i_0 [A]	μ_{max} [s^{-1}]
I	'metal-to-metal'	*K*	0.02	0.5	$3.74 \cdot 10^5$	1168	1.5	+6.23
II	hard vulc. rubber	*K*	0.02	0.5	$3.74 \cdot 10^5$	1168	1.5	–3.26
III	hard vulc. rubber	*K/2*	0.03	0.8	$0.649 \cdot 10^5$	779	1.0	–10.98
IV	soft polymer foil	*K/2*	0.03	0.8	$0.649 \cdot 10^5$	779	1.0	–36.13
V	soft polymer foil	*K/2*	0.04	0.8	$0.365 \cdot 10^5$	584	0.75	–14.57
VI	soft polymer foil	*K/2*	0.05	0.8	$0.234 \cdot 10^5$	467	0.6	–2.27

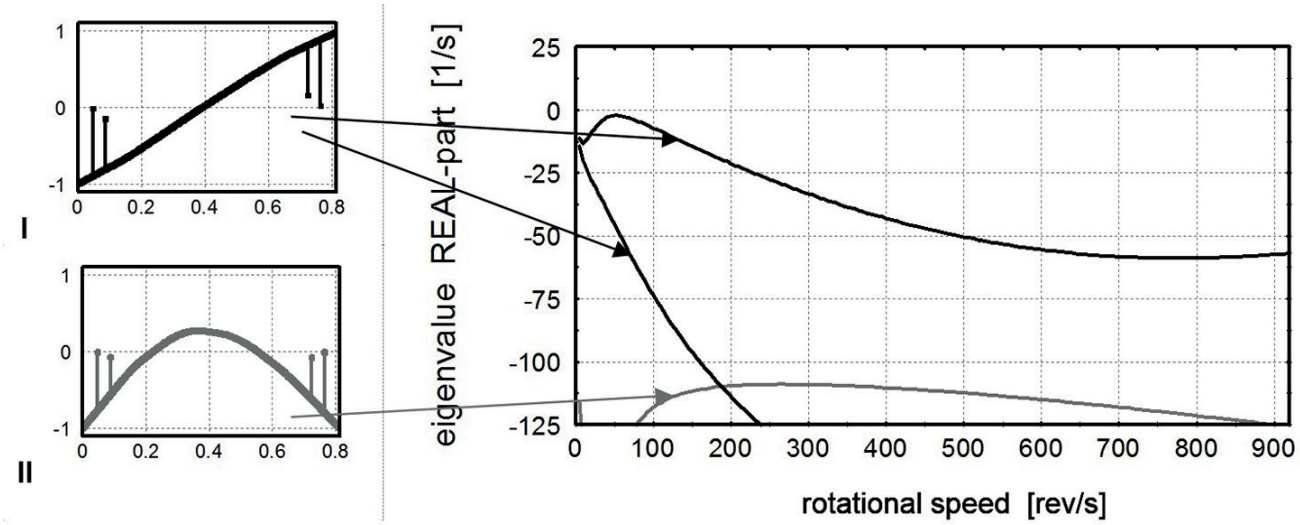

Fig. 14. Eigenvalue real parts determined for $t_r = 0.05$ s and $\gamma = 0.8$

The third column, entitled 'Global stiffness', corresponds to respective sets of stiffness and damping coefficients k_{xx}, k_{yy}, k_{xy}, k_{yx}, d_{xx}, d_{yy}, d_{xy}, and d_{yx} of the EDPMBs (see Fig. 9d). Numerical values of these quantities correspond to global stiffness K or $K/2$, as per expressions (2) and (3). In the subsequent columns, i.e. from the fourth to the seventh one, the AMD control parameters t_r and γ are inserted, respectively, as along with the coefficients of additional stiffness k_A and damping c_A. In the eighth column, the Table also contains the respective damper working point currents i_0 case by case. The final stabilization results expressed by maximum eigenvalue real parts $\mu_{\max}$ of the system eigenmodes, which are most sensitive to instability, have been inserted into the ninth column of Table 1.

From a mutual comparison of these values, it follows that for a reasonably selected global stiffness K of the EDPMBs as well as for their bushings embedded in layers made of relatively soft and viscous materials one obtains an entire stabilization effect of the rotor-shaft for the gradually lower and lower values of additional stiffness k_A and damping coefficients c_A introduced into both bearing supports. For this purpose, AMDs of reasonably small dimensions and low control energy consumption can be used. Namely, in example VI in Table 1 numerical values of k_A and c_A have been reduced, respectively, to $0.234 \cdot 10^5$ N/m and 467 Ns/m only. Here, in order to generate sufficient control gains to stabilize the object, it was possible to minimize the applied control current 2.5 times, i.e. from $i_0 = 1.5$ A to 0.6 A. This last case has been illustrated in the form of eigenvalue real part characteristics presented in Fig. 14.

7. Benefits following from application of EDPMBs combined with AMD

From the considerations performed above, it follows that, on the one hand, the EDPMBs have several advantages in a comparison with the classical AMBs, but on the other hand, such passive magnetic suspensions had to be stabilized by means of additional magnetic dampers which operate using a principle of the active magnetic bearing. Since complete AMBs can serve not only as rotor-shaft supports, but also as controllable vibration dampers, an indication of benefits following from application of the proposed combined solution seems to be worth considering. For this purpose, it is necessary to compare directly the proposed magnetic suspension consisting of the EDPMB and the AMD with a complete AMB designed to support the investigated laboratory rotor-shaft presented in Fig. 1. In addition to smaller weight and geometrical dimensions as well as much easier and robust control of the EDPMB combined with the AMD, the electric energy consumption expected from both solutions is going to be an essential criterion of this comparison. Here, two aspects of electric power consumption will be studied: during static operation under gravitational load only and in order to satisfy dynamic stability limits estimated by means of the Routh-Hurwitz criterion.

Despite the instability caused by the skew-symmetric visco-elastic properties, above certain rotational speeds the EDPMB self induces carrying forces without a need of external energy supply. However, in the case of a classical AMB its ability to balance static loads is determined by the force value F_0 corresponding to the bearing working point which is a function of the working point current i_0. If half the weight of the laboratory rotor-shaft, regarded as a symmetrical one, is balanced by the AMB in one (vertical) plane, the following well-known linearized relationship has to be satisfied:

$$F_0 = mg = \frac{\mu_0 N^2 A}{4} \frac{i_0^2}{x_0^2}, \tag{15}$$

where μ_0 is the magnetic permeability in a vacuum, N denotes the number of bearing coil windings, A is the electromagnet cross-section, x_0 denotes the nominal bearing clearance, m denotes the part of the rotor-shaft mass supported by a given bearing and g denotes gravitational acceleration. It turns out that for $\mu_0 = 1.2566 \cdot 10^{-6}$ H/m and for the complete AMB

with $N = 220$, $A = 9.0678 \cdot 10^{-5}$ m^2 and $x_0 = 0.0004$ m, designed for the considered laboratory rotor-shaft of the total mass $2m = 7.3$ kg, the working point current i_0 determined from (15) is equal to 2.04 A. Nevertheless, in order to assure sufficient controllability of this AMB, e.g. against dynamic overloadings due to residual unbalances, the working point current i_0 must be of at least two times greater value. Then, for the finally assumed $i_0 = 4$ A and for the bearing coil windings resistance of 0.85 Ω, such active magnetic suspension consumes electric power of 13.6 W in the one, i.e. vertical, plane. Here, the same working point current has to be set in the bearing horizontal plane. According to the above, the entire power consumption of such two AMBs supporting the considered rotor-shaft would be equal to $2\times(13.6 + 13.6) = 54.4$ W.

In the case of combined magnetic support proposed in this paper, in the vertical and horizontal plane the AMD introduces additional stiffness and damping coefficients which for the PD controller can be expressed as functions of the working point current i_0:

$$k_A = \frac{\mu_0 N^2 A}{4} \frac{i_0}{x_0^2}\left(P - \frac{i_0}{x_0}\right) \quad \text{and} \quad c_A = \frac{\mu_0 N^2 A}{4} D \frac{i_0}{x_0^2}, \tag{16}$$

where P and D denote the proportional and derivative control gains, respectively. Properly selected numerical values of these gains become fundamental parameters of the AMDs responsible for rotor-shaft stabilization with respective electric energy consumption ratios. For this purpose, and for the above-mentioned accuracy tolerance ratio $\beta = 0.04$, an appropriate combination of equations (13) and (16) together with (14) leads to the following relationship between the proportional and derivative gains:

$$P = \frac{1.6}{t_r \gamma^2} D + \frac{i_0}{x_0}. \tag{17}$$

If the considered active device acts as a classical carrying AMB, like the one mentioned above, with the working point current $i_0 = 4$ A and the above-listed damping coefficient value $c_A = 1168$ Ns/m, the corresponding derivative gain determined using (16) is equal to $D = 8.471$ As/m. Then, for $t_r = 0.02$ s and $\gamma = 0.5$ the proportional gain calculated by means of (17) is equal to $P = 1.2711 \cdot 10^4$ A/m, which results in the bearing radial 'in-plane' stiffness $k_A = 3.74 \cdot 10^5$ N/m. This stiffness value of both AMBs supporting the considered rotor-shaft assures its vertical displacement error of less than 0.1 mm caused by the gravitational load. When this active device acts as an AMD, however, the same values of c_A and k_A can be obtained for the essentially smaller working point current $i_0 = 1.5$ A, i.e. the same as in examples I and II contained in Table 1. Then, the corresponding control gains determined using (16) and (17) are equal to $D = 22.6$ As/m and $P = 1.0979 \cdot 10^4$ A/m. From the viewpoint of stabilization effectiveness, it is worth noting that while the damping coefficient c_A increases linearly with the working point current i_0, the stiffness value k_A is a parabolic function of i_0, as it follows from expressions (16) and (17) as well as from the respective plots in Fig. 15a. The electromagnetic stiffness values illustrated in this Figure for both proportional gain values are always positive. Here, it needs to be remembered that in addition to the supplementary damping activity, this feature of the 'in-plane' stiffness generated by the AMD has an essential positive influence on stabilization of the EDPMB. According to the above, in example II listed in Table 1, when the rotor-shaft has been successfully stabilized with the working point current $i_0 = 1.5$ A, the analogous power consumption of this active device operating as an AMD with coil windings resistance of 0.85 Ω amounts to $2\times(1.9125 + 1.9125) = 7.65$ W for two supports in two mutually perpendicular planes.

In the remaining examples of successful rotor-shaft stabilization listed in Table 1, i.e. in III–VI, achieved for gradually decreasing working point currents, all additional damping coefficient values c_A have been obtained for the same derivative gain value $D = 22.6$ As/m. However, the corresponding proportional gains determined by means of relation (17) were equal, respectively, to $P = 4383.35$ A/m in examples III and IV for

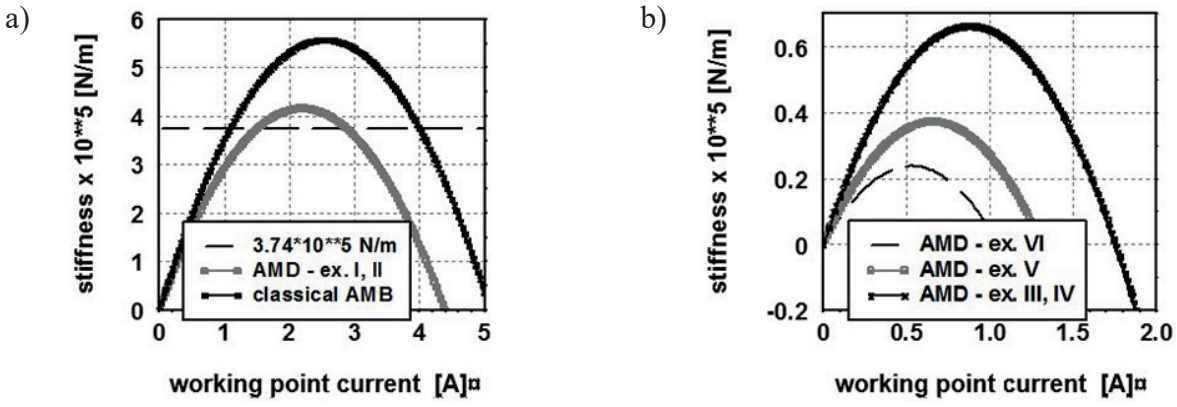

Fig. 15. Characteristics of stabilizing additional stiffness coefficients k_A determined for $P = 1.2711 \cdot 10^4$ and $P = 1.0979 \cdot 10^4$ A/m (a) and for $P = 4383.35$, $P = 3286.91$ and $P = 2629.04$ A/m (b)

$i_0 = 1.0$ A, $P = 3286.91$ A/m in example V for $i_0 = 0.75$ A and $P = 2629.04$ A/m in example VI for $i_0 = 0.6$ A. The analogous characteristics of the stabilizing additional stiffness coefficients k_A determined for these examples are depicted in Fig. 15b. This is to emphasize that in all these three cases maxima of the positive stiffness values generated by the AMDs correspond to the above-mentioned working point currents, which assures additional optimum influence on the rotor-shaft stabilization effect. The corresponding electric power consumption ratios are equal, respectively, to 3.4 W in examples III and IV, 1.9 W in example V, and 1.2 W in example VI, each for two considered AMDs acting in two planes. These wattages correspond, respectively, to 6.25, 3.5 and 2.2% of the consumption determined for the rotor-shaft supported on the carrying classical AMBs.

It needs to be remembered that the above-listed relatively small values of working point currents and electric power consumption ratios in examples III–VI corresponding to them have been achieved using an active device with technical parameters of the classical carrying AMB, i.e. with the above-mentioned number of bearing coil windings N, electromagnet cross-section A and nominal bearing clearance x_0. From formulae (16) it follows that for respectively the same working point currents i_0 identical values of stiffness k_A and damping coefficients c_A could be obtained for different technical parameters N, A and x_0 and for appropriately different gains P and D. Here, in order to minimize, for example, dimensions of the AMD cooperating with the EDPMB, it would be necessary to decrease the number of coil windings N, the electromagnet cross-section A as well as nominal clearance x_0. Then, the corresponding gains P and D should be appropriately greater, but not exceeding given realistic admissible values. According to the above, a design of EDPMBs stabilized by the AMDs requires selection of optimum interdependencies between the above-analyzed technical and control parameters of the active device.

8. Final remarks

In the paper, stabilization of a laboratory rotor-shaft supported by electro-dynamic passive magnetic bearings has been performed by means of three approaches applied simultaneously: by introduction of additional damping, using an efficient source of energy dissipation in the form of the active magnetic dampers built into the EDPMBs; by proper selection of the global stiffness value of the EDPMB, and by selection of optimum visco-elastic properties of bearing supports in housings. The magnitudes of the additional external damping necessary to stabilize the object under consideration have been assessed using the Routh-Hurwitz stability criterion, which can be regarded as a very useful although approximate indicator for stabilization of rotating systems. From the results of eigenvalue analyses, it follows that the additional damping coefficient values determined by means of this criterion for the system eigenmodes most sensitive to instability proved to be very effective for total stabilization of the investigated object. Moreover, it turned out that the softer the electrodynamic passive magnetic bearing as well as the softer and more viscous the bearing support in housings, the smaller AMD gains are required to stabilize the rotor-shaft completely. Although, by means of the technical treatments applied here, all bending eigenmodes of this high-speed rotor-shaft have been efficiently stabilized, it is hoped that an appropriate mutual balance between these three stabilization possibilities will be achieved in future research by means of a proper optimization procedure. It is also worth noting that the EDPMB stabilized by the properly designed AMD consumes noticeably less electric power than an alternative classical AMB. It should be emphasized that the computational findings described above are going to be used for final design of the test-rig which will enable numerous necessary experimental verifications of the assumed theoretical model of the investigated rotor-shaft supported by electrodynamic passive magnetic bearings.

Acknowledgements. The investigations were supported by the Polish National Centre for Research and Development, Research Project PBS1/B6/7/2012.

References

[1] A.V. Filatov, E.H. Maslen, and G.T Gillies, "A method of non-contact suspension of rotating bodies using electromagnetic forces", *Journal of Applied Physics*, Vol. 91, 2355–2371 (2002).

[2] A.V. Filatov, E.H. Maslen, and G.T. Gillies, "Stability of an electrodynamic suspension", *Journal of Applied. Physics*, Vol. 92: 3345–3353 (2002).

[3] T.A. Lembke, *Design and analysis of a novel low loss homopolar electrodynamic bearing*, Doctoral Thesis, KTH Electrical Engineering, Stockholm, 2005.

[4] T. Szolc and K. Falkowski, "Dynamic analysis of the high-speed flexible rotors supported on the electrodynamic passive magnetic bearings", *Mechanisms and Machine Science*, Springer Verlag, Vol. 21: 1489–1500 (2015).

[5] N. Amati, X. De Lépine, and A. Tonoli, "Modeling of electrodynamic bearings", *ASME Journal of Vibration and Acoustics*, Vol. 130: p. 061007 (2008).

[6] J.G. Detoni J., F. Impinna, A. Tonoli, and N. Amati, "Unified modeling of passive homopolar and heteropolar electrodynamic bearings", *Journal of Sound and Vibration*, 331, 4219–4232 (2012).

[7] P. Cui, J. He, J. Fang, X. Xu, J. Cui, and S. Yang, "Research on method for adaptive imbalance vibration control for rotor of variable-speed mscmg with active-passive magnetic bearings", *Journal of Vibration and Control*: 1–14, (2015) DOI: 10.1177/1077546315576430

[8] J. Sandtner and H. Bleuler, "Electrodynamic passive magnetic bearing with planar Halbach arrays", *Proc. of the 9th Int. Symposium on Magnetic Bearings*, Lexington, Kentucky, USA (2004).

[9] F. Impinna, J.G. Detoni, A. Tonoli, N. Amati, and M.P. Piccolo, "Test and theory of electrodynamic bearings coupled to active magnetic dampers", *Proc. of the 14th Int. Symposium on Magnetic Bearings*, Linz, Austria, 263–268 (2014).

[10] Q. Cui, "Stabilization of electrodynamic bearings with active magnetic dampers", Doctoral Thesis No. 7334, École Polytechnique Fédérale de Lausanne (2016).

[11] J.G. Detoni, F. Impinna, N. Amati, A. Tonoli, M.P. Piccolo, and G. Genta G., "Stability of a 4 degree of freedom rotor on electrodynamic passive magnetic bearings", *Proc. of the 14th Int. Symposium on Magnetic Bearings*, Linz, Austria, Vol. 14 (2014).

[12] X. Sun, B. Su, L. Chen, Z. Yang, and K. Li, "Design and analysis of interior composite-rotor bearingless permanent magnet synchronous motors with two layer permanent magnets", *Bull. Pol. Ac.: Tech.*, Vol. 65, No. 6, 833–843 (2017).

[13] T. Szolc, "On the discrete-continuous modeling of rotor systems for the analysis of coupled lateral-torsional vibrations", *International Journal of Rotating Machinery*, 6(2), 135–149 (2000).

[14] T. Szolc, P. Tauzowski, R. Stocki, and J. Knabel, "Damage Identification in Vibrating Rotor-Shaft Systems by Efficient Sampling Approach", *Mechanical Systems and Signal Processing*, Vol. 23: 1615–1633 (2009).

[15] R. Lasota, R. Stocki, P. Tauzowski, and T. Szolc, "Polynomial chaos expansion method in estimating probability distribution of rotor-shaft dynamic responses", *Bull. Pol. Ac.: Tech.*, Vol. 63, No. 1, 413–422 (2015).

[16] G. Genta, Dynamics of Rotating Systems, Springer Science + Business Media, Inc. (2005)

[17] R.C. Dorf and R.H. Bishop, Modern Control Systems, Prentice Hall, The Twelfth Edition (2011).

[18] M. Henzel and P. Mazurek, "The rapid prototyping of active magnetic bearing", *Advances in Intelligent Systems and Computing, Recent Advances in Automation, Robotics and Measuring Techniques*, Springer, Vol. 267, 155–166 (2014).

[19] E. Prut, T. Medintseva, and V. Dreval, Mechanical and rheological behavior of unvulcanized and dynamically vulcanized i-PP/EPDM Blends, Volume233, Issue1, Special Issue: Fillers, Filled Polymers and Polymer Blends (2006).

[20] T.A. Osswald and N. Rudolph, Polymer Rheology. Fundamentals and Applications, Hanser Publisher, Munich (2014), ISBN: 978–1–56990–517–3.